Effect of Synthesis Parameters of Graphene/Fe_2O_3 Nanocomposites on Their Structural and Electrical Conductivity Properties

A. Jedrzejewska[a,*], D. Sibera[a], U. Narkiewicz[a], R. Pełech[b] and R. Jedrzejewski[c]

[a]Institute of Chemical and Environment Engineering, Faculty of Chemical Engineering, West Pomeranian University of Technology, gen. K. Pułaskiego 10, 70-322 Szczecin, Poland

[b]Institute of Organic Chemical Technology, Faculty of Chemical Engineering, West Pomeranian University of Technology, gen. K. Pułaskiego 10, 70-322 Szczecin, Poland

[c]Institute of Materials Science and Engineering, Faculty of Mechanical Engineering and Mechatronics, West Pomeranian University of Technology, al. Piastów 19, 70-310 Szczecin, Poland

(Received 26 June 2017; in final form 16 August 2017)

Due to its fascinating properties such as high surface area, very good electrical and thermal conductivity, excellent mechanical properties, optical and electrochemical properties, graphene may be the ideal material as a substrate of nanocomposites for applications in electronics. Graphene layer can be used as a conductive matrix allowing good contact between crystallites of nanomaterials. Despite pure graphene, its composites with other species can be of interest. In this paper the results of studies on the effect of methods and parameters of synthesis, for obtaining composites graphene/Fe_2O_3 on their structural properties and electrical properties are presented. A series of experiments was conducted using a commercially available graphene (Graphene Nanopowder AO-3) and iron nitrate. The materials were obtained using two pressure methods: pressure synthesis in the autoclave and synthesis in the microwave solvothermal reactor. The syntheses were carried out in a solution of ethanol. The specific surface area, helium density, morphology, phase composition, thermal properties and electric conductivity of the obtained composites were investigated.

DOI: 10.12693/APhysPolA.132.1424

PACS/topics: 61.48.Gh, 65.80.Ck, 81.07.Bc

1. Introduction

Graphene is composed of a single layer of carbon atoms which form six-membered linked rings. The length of the bonds between carbon atoms is about 0.0142 nm. Graphene has exceptional properties. It is over two hundred times tougher than steel of the same thickness and simultaneously it is extremely flexible. It can be smoothly stretched by 20%, the elastic limit is in the range of 1 TPa, and the Young modulus is equal to 0.5 TPa. Measurements of thermal conductivity of graphene gave the results ranged from 4840±440 to 5300±480 W/mK. The resistivity of graphene is very low, only 10^{-8} Ωm. Chemical modification can transform graphene into an almost perfect insulator. Graphene is also almost transparent material (absorbs only 2.3% of light). Such exceptional properties of graphene allow its use in electronic industry, energy sector and medicine [1–4].

Taking into account the interesting properties mentioned here above, combining graphene with other compounds containing appropriate functional groups, as metal oxides, and introducing them into a polymer matrix, one can obtain composites with new, interesting features, absent in the component materials considered separately [5]. Ferrites seem to be excellent candidates as additives to obtain magnetic composites based on graphene. Soft ferrites, as $NiFe_2O_4$ are mixtures of metal oxides of general formula MFe_2O_4 (M = bivalent metal ion, e.g. Ni, Co, Cu), and they are one of the most attractive groups of magnetic materials, commonly used in microwave devices, data carriers or antenna rods [6–8]. This class of materials makes also use of their multifunctional properties, as various redox states and electrochemical stability [9], which makes them ideal candidates for catalytic/photocatalytic application [10, 11], devices for electrochemical energy storage [12, 13] and gas/humidity sensors [14].

Fe_2O_3, which is an abundant, cost-effective and environmentally benign n-type semiconductor with bandgap of 2.2 eV, has been extensively studied because of its peculiar and fascinating physicochemical properties and wide potential applications in diverse fields. Fe_2O_3 has been intensively investigated as a promising anode material for LIBs (lithium ion battery) owing to its high capacity, abundance, environmental benignity, and low cost. Compared to other transition metals and metal oxides, Fe_2O_3 is an attractive anode material for LIBs due to its high theoretical capacity (1007 mAh/g). Recently, Fe_2O_3 has been used to form hybrid materials

*corresponding author; e-mail: Anna.Jedrzejewska@zut.edu.pl

with graphene nanostructures for lithium ion batteries. However, Fe_2O_3 used as electrode material suffers from poor cycling performance caused by its low electrical conductivity and large volume changes (> 200%). During the lithiation/delithiation processes and subsequent pulverization of particles a structural degradation of electrode material occurs. Therefore, further studies on the electrical properties of graphene/Fe_2O_3 composites are necessary [15, 16].

In the literature many methods have been described for preparing nanocomposites graphene/Fe_2O_3. These processes are carried out in stages. In a first step, the slurry graphene oxide in water, ethanol or acetone is subjected to sonication. Then into the mixture there is added iron salt (nitrate, chloride or acetate). In the next step for the mixture there is added a substance enhancing the pH (sodium, potassium or ammonium) for preparing hydroxide precipitation of iron. The final stage of preparation involves placing the mixture in an autoclave or other pressure device to carry out the pressure process for 8–24 h. After autoclaving the material is often annealed in a furnace at 500 °C under an atmosphere of an inert gas (nitrogen, argon) [5, 6, 17–21]. Zhu Xianjun described in his work a method of obtaining nanocomposite graphene/Fe_2O_3 using microwaves. In the first preparation step a mixture of graphene oxide with iron chloride and urea at a temperature of 90 °C was prepared. After cooling to room temperature, there to hydrazine was added in a commercial microwave equipment. After the microwave treatment the formation of a composite graphene/Fe_2O_3 was confirmed using such methods as X-ray diffraction (XRD), X-ray photoelectron spectroscopy (XPS), scanning electron microscopy (SEM), and transmission electron microscopy (TEM). However, in commercially available microwave equipment it is not possible to generate and maintain a constant pressure as high as in a microwave reactor used by the authors of the above operation [22].

In this work, we report an easy and quick way of synthesizing graphene/Fe_2O_3 nanocomposite by impregnation carried out in microwave solvothermal reactor and autoclave. In addition, there will be examined the effect of synthesis parameters on the electrical properties of the composites.

2. Experimental

2.1. Preparation of nanocomposites graphene/Fe_2O_3

Graphene/Fe_2O_3 hybrid materials were synthesized by applying a microwave solvothermal reactor and an autoclave. At first, a mixture of graphene (we used commercially available graphene (Graphene Nanopowder AO-3)) in ethanol was obtained and ultrasonic sonification was carried out for 20 min. In next step iron nitrate and ammonia water were added to this solution and stirred. Then, the obtained solution was subjected to a pressure treatment. Pressure treatment in the autoclave was performed for time varied between 12 to 24 h (change every 4 h) and temperature varied between 120 °C to 200 °C (change every 40 °C). Pressure treatment in the microwave solvothermal reactor was much shorter, the solution was treated here for 15 to 45 min (change every 15 min), under a pressure of 40 to 50 atm (change every 5 atm).

Using these procedures we obtained a nanocomposite material graphene/$n$$Fe_2O_3$ (n = 25 wt%). Next, the obtained materials were filtered and washed with deionised water to remove salt residues. Finally, the materials were dried at 80 °C for 24 h.

2.2. Methods of characterisation

The specific surface area σ of the obtained samples was determined by physical adsorption of N_2 at –196 °C using Quantachrome Quadrasorb Instruments. Helium density ρ measurements were made on the Micro-Ultrapyc 1200e. Morphology of nanocomposites was investigated using TEM (FEI TECNAI G2 F-20 S TWIN). The effect of the synthesis parameters on the phase composition of the samples obtained was examined by using XRD on the Empyrean apparatus of PANalytical. The thermal properties of nanocomposites were determined on the basis of DTA-Q600 SDT TA Instruments thermal imaging. Electric conductivity was determined by measuring the resistivity using the Van der Pauw method of a 10%w/w of material in paraffin plate.

3. Results and discussion

3.1. XRD analysis

The structure and crystallinity was determined by a powder XRD studies using a PANalytical Empyrean X-ray diffractometer. Cu K_α radiation with wavelength λ = 1.54 Å was used for the study. The obtained XRD pattern was analyzed in the X'Pert High Score Plus program using the ICDD PDF-4+ database. Phase analysis and calculation of the average size of Fe_2O_3 phase crystallites were made for samples prepared in the microwave reactor and autoclave. The reaction medium was ethanol.

As shown in Fig. 1, peaks shown on the nanocomposite pattern can be ascribed to the well-crystallized (average crystallites size: 63±3 nm) rhombohedral phase of Fe_2O_3 structure (ICDD 00-024-0072) and graphite phase with a characteristic peak at $2\Theta = 26.52°$, indicating an interlayer spacing of 0.336 nm with an index of (002). Some small peaks of carbon (ICDD 00-026-1076) can be identified as well. Stacking peak of graphene sheets could indicate that the agglomeration in the hybrid material still occurred and graphite-like structure is formed.

The analysis of XRD patterns made for samples prepared at 40, 45, and 50 atm for various reaction times (15–45 min) showed that all composites had the same phase composition. Analysis of patterns for autoclaved materials showed that concerning the phase composition, they did not differ from the composites made in the microwave reactor. It is shown in Fig. 2 illustrating the

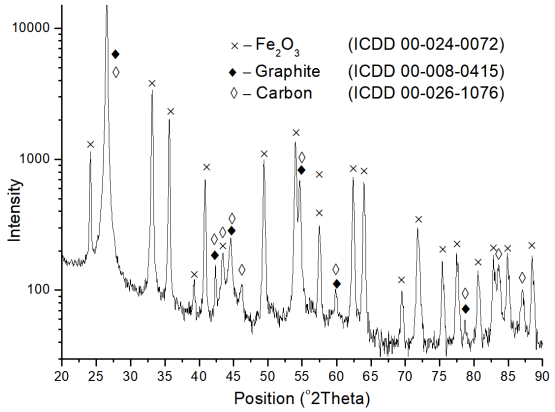

Fig. 1. XRD pattern of the composite obtained in the microwave reactor in ethanol at 40 atm, reaction time 15min.

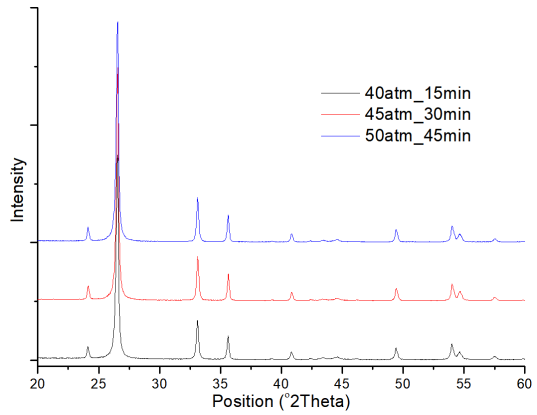

Fig. 2. Compilation of XRD spectra of composites obtained in a microwave reactor in ethanol at different pressures and at different reaction times of 15-45 min.

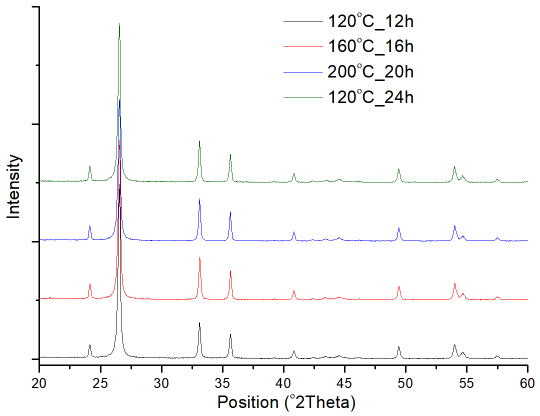

Fig. 3. Composition of XRD spectra of composites obtained in an autoclave in ethanol at different temperatures and at different reaction times of 12-24 hours.

patterns for composites obtained in the microwave reactor and in Fig. 3 showing an example of composites prepared in the autoclave.

3.2. Structural analysis

The textural properties of the graphene composites were determined by physical adsorption of N_2 at –196 °C using a Quadrasorb apparatus. Specific surface area was measured by the multi-point Brunauer–Emmett–Teller (BET) equation [23] method with the N_2 adsorption isotherm over a relative pressure (P/P_0) in the range of 0.05–0.20. The total pore volume, V_p, which including both micropores and mesopores, was estimated by converting the amount of N_2 gas adsorbed at a relative pressure of 0.99 to liquid volume of the adsorbate (N_2). Micropore volumes (< 2 nm), V_{mic}, and determined using the density functional theory (DFT). All samples were degassed using vacuum at 250 °C for 16 h prior to each measurement. The results are shown in Table I and Table II.

TABLE I

Structural parameters for obtained materials in the microwave solvothermal reactor.

Sample	σ [m^2/g]	V_p [cm^3/g]	V_{mic} [cm^3/g]	ρ [g/cm^3]
graphene	64	0.1096	0.0201	1.7763
40 atm/15 min	45	0.1232	0.0133	2.4430
40 atm/30 min	43	0.1144	0.0123	2.4211
40 atm/45 min	43	0.1233	0.0126	2.4907
45 atm/15 min	44	0.1145	0.0131	2.4377
45 atm/30 min	48	0.1068	0.0136	2.4849
45 atm/45 min	46	0.1024	0.0132	2.4998
50 atm/15 min	48	0.0987	0.0147	2.4671
50 atm/30 min	46	0.1086	0.0132	2.4122
50 atm/45 min	44	0.1109	0.0129	2.4063

TABLE II

Structural parameters for materials obtained in the autoclave.

Sample	σ [m^2/g]	V_p [cm^3/g]	V_{mic} [cm^3/g]	ρ [g/cm^3]
graphene	64	0.1096	0.0201	1.7763
120 °C/12h	41	0.0962	0.0112	2.3831
120 °C/16h	37	0.0914	0.0207	2.3804
120 °C/20h	42	0.0976	0.0119	2.3631
120 °C/24h	40	0.0937	0.0114	2.3980
160 °C/12h	37	0.0931	0.0134	2.3486
160 °C/16h	35	0.0952	0.0098	2.4034
160 °C/20h	26	0.0809	0.0069	2.3723
160 °C/24h	37	0.0955	0.0117	2.3858
200 °C/12h	35	0.0874	0.0100	2.3897
200 °C/16h	36	0.0846	0.0115	2.3727
200 °C/20h	39	0.1008	0.0124	2.4418
200 °C/24h	40	0.0962	0.0118	2.3672

TABLE III

The results of the conductivity, where $G = \frac{1}{\rho}$.

Sample	G [S/m]	Sample	G [S/m]
graphene	0.59	graphene	0.59
40 atm/15 min	0.12	120 °C/12h	0.018
40 atm/30 min	0.079	120 °C/16 h	0.14
40 atm/45 min	0.011	120 °C/20 h	2.4
45 atm/15 min	0.11	120 °C/24 h	0.066
45 atm/30 min	0.092	160 °C/12 h	0.034
45 atm/45 min	0.092	160 °C/16 h	0.012
50 atm/15 min	0.2	160 °C/20 h	0.2
50 atm/30 min	0.15	160 °C/24 h	0.19
50 atm/45 min	0.16	200 °C/12 h	0.049
		200 °C/16 h	non-conducting
		200 °C/20 h	non-conducting
		200 °C/24h	non-conducting

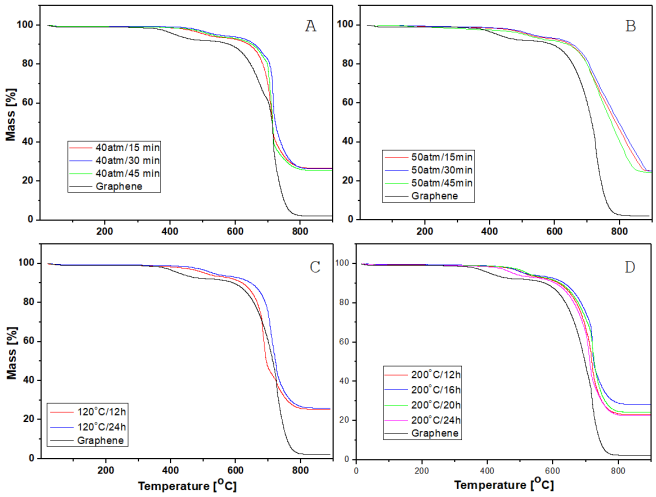

Fig. 4. Tg curves of selected samples.

Data presented in Table I and Table II show that all samples have lower surface area than pure graphene which is due to the fact that that iron oxide covers the surface graphene. In addition, the BET results, pore content and content of micropores are quite similar for all materials, regardless the synthesis method and the synthesis parameters. Small changes depend on the properties of the starting and on locations of Fe_2O_3 particles.

Results of helium density measurements are shown in Table I and Table II. It can be concluded that all tested samples have higher density than the pure graphene sample. This is due to the presence of Fe_2O_3 in the samples since its density in the literature is 5.24 g/cm^3. In addition, the density of all measured samples is at a comparable level. This is due to the fact that in all samples the amount of iron oxide was the same. Minor differences may result from varying degrees of crystallisation of iron oxide depending on synthesis parameters and slight differences in Fe_2O_3 content in samples resulting from losses in the synthesis process.

Thermal properties of nanocomposites were determined by thermogravimetric analysis. The results of the selected samples are shown in Fig. 4a–d. The tested materials exhibited thermal stability up to about 400 °C. The weight loss below this temperature was due to the evaporation of water from the surface and from the pores of the materials. In all tested samples, the course of thermogravimetric curves is similar. From the analysis of thermogravimetric curves, the mass loss of the tested composites started after exceeding 400 °C. It was due to the gasification of carbon and the removal of the resulting carbon oxides [24, 25]. Above 600 °C the weight loss reached 7.5%, which could result from detachment of oxygen installed on graphene surface. Carbon gasification process ended at 830 °C. The total weight loss was about 74–75%, than the remaining material is composed of Fe_2O_3 only. The weight loss in the range of 74–75% also confirmed the intended composition of the obtained composites –75 wt% of carbon and 25 wt% of Fe_2O_3. The previously analyzed XRD spectra also confirmed that the samples consisted only of carbon and Fe_2O_3. Similar TG curves were observed by other researchers, but our materials exhibited the highest weight loss at higher temperature, indicating for better thermal stability of the obtained composites [15, 26].

3.3. TEM analysis

Microstructure and morphology of obtained products were further characterized by TEM technique. TEM images in Fig. 5 show the morphology of various graphene/Fe_2O_3 samples obtained in microwave solvothermal reactor. All the samples graphene/Fe_2O_3 exhibit a typically wrinkled, sheet-like structure. Fe_2O_3 nanoparticles with the average particle size less than 100 nm were rather uniformly distributed on the graphene sheets. The average crystallite size was calculated manually from the pictures.

3.4. Electrical properties

Electrical properties were determined by measuring the resistivity of the layer containing the test material dispersed in paraffin. Samples were made by adding 100 mg of the test powder to 1 g of molten paraffin. The suspension of powder in paraffin was placed in an ultrasonic bath, and the ultrasound power was adjusted to solidify it in the molds of polypropylene.

The results of electrical properties are shown in Table III. Below there is a schematic diagram of the system applied to carry out the measurements (Fig. 6). The thickness of the sample was determined with a micrometer screw. The resistivity of the materials was determined numerically from the van der Pauw equation [27].

Resistance was determined from the equation van der Pauw [27, 28]:

$$\exp\left(\frac{-\pi R_{21,43} d}{\rho}\right) + \exp\left(\frac{-\pi R_{23,41} d}{\rho}\right) = 1,$$

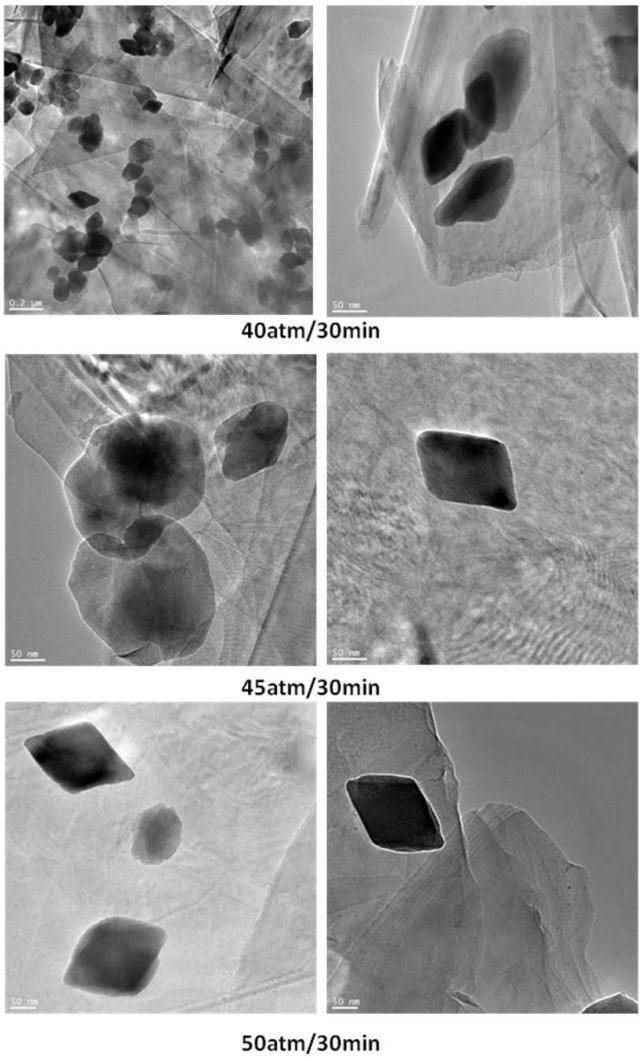

Fig. 5. TEM images of samples obtained in microwave solvothermal reactor and autoclave.

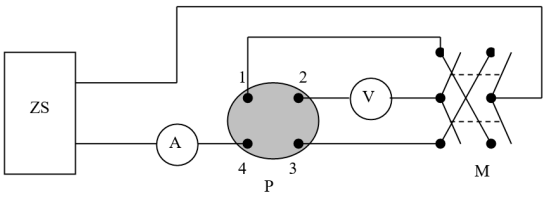

Fig. 6. 1, 2, 3, 4 — measurement contacts, M — bridge H, P — sample of tested material, ZS — power supply stabilized.

where

$$R_{21,43} = \frac{U_{21}}{I_{43}}, \quad R_{23,41} = \frac{U_{23}}{I_{41}},$$

U_{21} — voltage drop between contacts 2–1 [V], U_{23} — voltage drop between contacts 2–3 [V], I_{43} — current flow between the contacts 4–3 [A], I_{41} — current flow between the contacts 4–1 [A], d — sample thickness [m], ρ — resistivity [Ωm].

It was found that test samples filled with the modified material had lower electrical conductivity comparing to the unmodified graphene. In addition, both the elongation of reaction time and the application of tougher conditions (temperature rise and pressure) led to further reduction of the conductivity. These results indicate that the applied method allowed us to effectively decorate graphene surface with Fe_2O_3 nanoparticles.

4. Conclusions

Graphene/Fe_2O_3 composites were successfully synthesized both in an autoclave and in the microwave solvothermal reactor. Structure, surface morphology and electrical properties of the graphene/Fe_2O_3 composites were investigated. XRD results have shown that all obtained materials were composites (no new phases were observed). According to thermogravimetric studies the prepared materials have a high thermal stability than pure graphene. On the contrary, studies of electrical properties have shown that composite samples had lower electric conductivity than pure graphene.

Acknowledgments

This work was supported by project: LIDER/496/L-6/14/NCBR/2015 financed by The National Centre for Research and Development.

References

[1] A.K. Geim, *Science* **324**, 1530 (2009).

[2] K.S. Novoselov, D. Jiang, F. Schedin, T.J. Booth, V.V. Khotkevich, S.V. Morozov, A.K. Geim, *Proc. Natl. Acad. Sci.* **102**, 10451 (2005).

[3] M.S. Fuhrer, *Nature* **459**, 1037 (2009).

[4] R.R. Nair, P. Blake, A.N. Grigorenko, K.S. Novoselov, T.J. Booth, T. Stauber, N.M.R. Peres, A.K. Geim, *Science* **320**, 1308 (2008).

[5] E. Kamali Heidari, B. Zhang, M. Heydarzadeh Sohi, A. Ataie, J.K. Kim, *J. Mater. Chem. A* **2**, 8314 (2014).

[6] S. Xuan, F. Wang, Y.X.J. Wang, J.C. Yu, K.C.F. Leung, *J. Mater. Chem.* **20**, 5086 (2010).

[7] J. Jacob, M.A. Khadar, *J. Appl. Phys.* **107**, 114310 (2010).

[8] S. Seifikar, T. Rawdanowicz, W. Straka, C. Quintero, N. Bassiri-Gharb, J. Schwartz, *J. Magn. Magn. Mater.* **61**, 255 (2014).

[9] J.L. Gunjakar, A.M. More, K.V. Gurav, C.D. Lokhande, *Appl. Surf. Sci.* **254**, 5844 (2009).

[10] K.S. Lin, A.K. Adhikari, Z.Y. Tsai, Y.P. Chen, T.T. Chien, H.B. Tsai, *Catal. Today* **174**, 88 (2011).

[11] E. Casbeer, V.K. Sharma, X.Z. Li, *Sep. Purif. Technol.* **87**, 1 (2012).

[12] L. Xu, J. Xia, H. Xu, S. Yin, K. Wang, L. Huang, L. Wang, H. Li, *J. Power Sources* **245**, 866 (2014).

[13] P. Xiong, H. Huang, X. Wang, *J. Power Sources* **245**, 937 (2014).

[14] K. Mukherjee, D.C. Bharti, S.B. Majumder, *Sens. Actuat. B* **146**, 91 (2010).

[15] G. Wang, T. Liu, Y. Luo, Y. Zhao, Z. Ren, J. Bai, H. Wang, *J. Alloys Comp.* **509**, 216 (2011).

[16] X. Zhu, Y. Zhu, S. Murali, M.D. Stoller, R.S. Ruoff, *ACS Nano* **5**, 3333 (2011).

[17] S. Guo, G. Zhang, Y. Guo, J. C. Yu, *Carbon* **60**, 437 (2013).

[18] L. Tian, Q. Zhuang, J. Li, C. Wu, Y. Shi, S. Sun, *Electrochim. Acta* **65**, 153 (2012).

[19] C. Wu, H. Zhang, Y. Wu, Q. Zhuang, L. Tian, X. Zhang, *Electrochim. Acta* **134**, 18 (2014).

[20] W. Yang, Z. Gao, J. Wang, B. Wang, L. Liu, *Solid State Sci.* **20**, 46 (2013).

[21] H. Li, Q. Zhao, X. Li, Z. Zhu, M. Tade, S. Liu, *J. Nanopart. Res.* **15**, 1670 (2013).

[22] J. Zhu, T. Zhu, X. Zhou, Y. Zhang, X.W. Lou, X. Chen, H. Zhang, H.H. Hng, Q. Yan, *Nanoscale* **3**, 1084 (2011).

[23] S. Brunauer, P.H. Emmett, E. Teller, *J. Am. Chem. Soc.* **60**, 309 (1938).

[24] L.L. Tian, Q.C. Zhuang, J. Li, C. Wu, Y.L. Shi, S.G. Sun, *Electrochim. Acta* **65**, 153 (2012).

[25] D.A. Dikin, S. Stankovich, E.J. Zimney, R.D. Piner, G.H.B. Dommett, G. Evmenenko, SonBinh T. Nguyen, R.S. Ruoff, *Nature* **448**, 457 (2007).

[26] M. Saraf, K. Natarajan, S.M. Mobin, *RSC Adv.* **7**, 309 (2017).

[27] L.J. van der Pauw, *Philips Res. Repts.* **13**, 1 (1958).

[28] Quantum Design Application Note 1076-304, Rev. A01, March 2007.